ChemComm

COMMUNICATION

View Article Online
View Journal | View Issue

Check for updates

Cite this: *Chem. Commun.*, 2020, **56**, 802

Received 28th November 2019, Accepted 10th December 2019

DOI: 10.1039/c9cc09279j

rsc.li/chemcomm

A black phosphorus-based cathode for aqueous Na-ion batteries operating under ambient conditions†

Jéssica E. S. Fonsaca,[a] Sergio H. Domingues,[b] Elisa S. Orth[a] and Aldo J. G. Zarbin*[a]

We present the unprecedented application of a black phosphorus-based nanocomposite as an electrode for aqueous Na-ion batteries under ambient conditions. An impressive specific capacity of up to 200 mA h g^{-1} was reached after 50 cycles in a NaCl aqueous solution used as a supporting electrolyte. Post-characterization indicated the integrity of the black phosphorus.

The interest in aqueous-based electrochemical energy storage devices has been growing, especially due to their inherent low cost and safety features. Aqueous batteries (ABs) are less sensitive to air and the high conductivity of the electrolyte may ensure faster charging/discharging processes than the nonaqueous ones.[1] The growing exploration of these systems is based on the intercalation-chemistry, which has emphasized intercalating cations such as Li^+, Na^+, K^+, Mg^{2+} and Zn^{2+}.[1] Indeed, Na-based electrolytes are very promising for large-scale applications, once sodium is truly abundant and economical,[2] being an alternative to the previously explored lithium-ion batteries. However, the large ionic radius of Na^+ (compared to Li^+) avoids the use of common materials as electrodes, which makes the search for new materials aiming at high Na^+ storage imperative. Recently, we reported impressive capacities of up to 150 mA h g^{-1} at 0.67 A g^{-1} for an aqueous Na-ion battery based on hexacyanometallates.[3] Black phosphorus (BP) has also recently begun to draw attention,[4,5] mainly due to its large interlayer distance, suitable for Na^+ intercalation.

BP has a layered structure held together by van der Waals interactions, similar to graphite, and each phosphorus atom is covalently bonded at the in-plane layer.[6] Many outstanding properties have been attributed to BP and its derivative.[7] Undoubtedly, its high theoretical specific capacity has placed this material in the spotlight of the energy field.[8] In fact, many works have reported BP as an efficient electrode for rechargeable ion batteries (*e.g.* K/Na/Li-ion) in an organic medium.[4,5] However, BP easily degrades on contact with oxygen, precluding its potential application.[9] Indeed, many authors have described the preparation of polymer-based nanocomposites aiming at BP protection against oxidation.[10,11] BP applications under mild conditions, such as in transistors,[12] photothermal devices,[13] humidity sensors[14] and others, have also been demonstrated.[15,16] Recently, we reported the synthesis of a composite of BP and polyaniline (BP-PANI) through a liquid–liquid (L/L) interfacial method, obtaining a free-standing, thin and transparent film.[17] PANI was shown to be an efficient degradation inhibitor, indicating an astonishing increase in BP lifetime under humidity and an oxygen atmosphere. Based on that, now we report the first example of a real potential application for this BP-PANI composite, as an electrode for aqueous Na-ion batteries, under ambient conditions. To the best of our knowledge, there are no experimental works considering BP-based materials as electrodes for aqueous batteries, or any application of a BP-based material working in water and ambient atmosphere. Mu Gu *et al.* have theoretically estimated a high efficiency for sodiation processes in BP-based cathodes, at around 536 mA h g^{-1}.[18]

A detailed experimental procedure is given in the ESI.† All electrochemical measurements were carried out in an aqueous solution of NaCl at pH 3, guaranteeing enough H_3O^+ ions to promote the redox processes of PANI, which stood out as the cathode for aqueous batteries.[19–21] The cyclic voltammograms of neat PANI and BP-PANI (Fig. 1A) presented two reversible redox processes, characteristic of the conducting polymer. The redox pairs A/A′ and B/B′ at around 0.15 and 0.50 V refer to the oxidation processes leucoemeraldine/emeraldine and emeraldine/pernigraniline, respectively. By comparing the profiles of the pure polymer with the composite, an increase in the current density, as well as a better definition and narrowing of the peaks, can be observed. This may imply a greater faradaic contribution and easier conversion of the processes after BP insertion. The cyclic voltammogram of pure BP can be seen in detail in Fig. 1B, which exhibits a defined process (C/C′) at 0.50 V, with very low current density. The attribution of this process becomes difficult since

---

[a] *Department of Chemistry, Federal University of Paraná (UFPR), CP 19032, CEP 81531-980, Curitiba, PR, Brazil. E-mail: aldozarbin@ufpr.br; Tel: +55 41-33613176*

[b] *Graphene and Nanomaterials Research Center, Mackenzie Presbyterian University, 01302-907, São Paulo, Brazil*

† Electronic supplementary information (ESI) available: Experimental details, and characterization of materials. See DOI: 10.1039/c9cc09279j

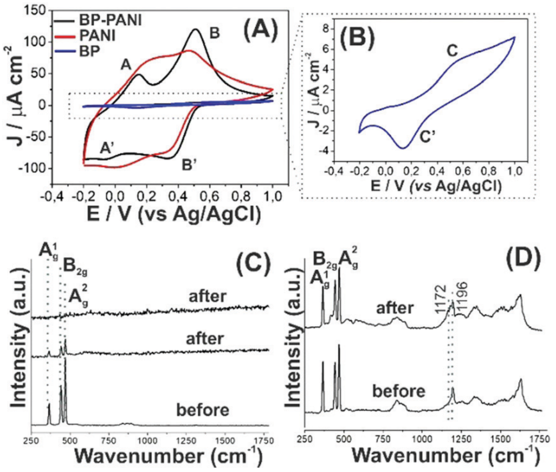

Fig. 1 (A) Cyclic voltammetry of BP, BP-PANI and PANI in NaCl 0.5 mol L^{-1} aqueous solution, pH 3, at 10 mV s^{-1}. (B) Detail of the neat BP voltammetric cycle (dashed area in (A)); (C and D) Raman spectra of BP and BP-PANI samples, respectively, before and after 200 voltammetric cycles.

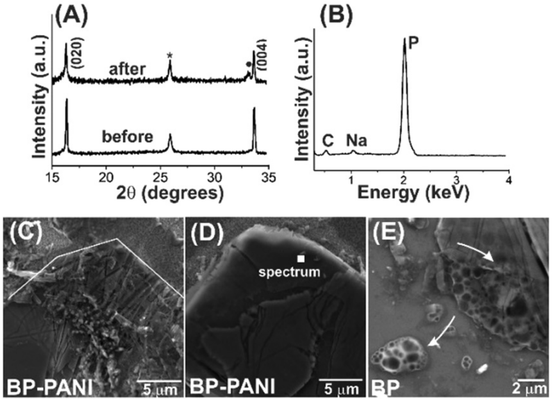

Fig. 2 (A) X-ray diffractograms of BP-PANI before and after 200 voltammetric cycles (* are related to the FTO substrates). (B) EDS spectrum and (C and D) SEM images of BP-PANI after 200 cycles; (E) SEM image of BP after 200 cycles.

the electrochemical characterization of BP in an aqueous medium has been poorly explored in the literature. Recently, Pumera *et al.*[22] reported the voltammetric characterization of BP in a phosphate buffer electrolyte with dissolved oxygen. The results attested the degradation of BP once an irreversible process at around 0.6 V (*vs.* Ag/AgCl), assigned to the oxidation of P to P(V), was verified. Here, pure BP shows a reversible process, indicating that a different process is occurring. It is known that BP has a large interlayer spacing, appropriate to accommodate Na^+ ions,[7] besides being able to electrochemically react with sodium to form a binary alloy.[23,24] Thus, the observed process could be related to any of these phenomena. Indeed, Sang Soo Han *et al.*[25] have verified, through first-principles calculations, that the sodiation mechanism may initially involve the intercalation/de-intercalation of Na^+ ions into the material lattice, followed by the alloying/de-alloying processes. To further investigate this system, samples were evaluated before and after 200 voltammetric cycles.

Fig. S1A and B (ESI†) presents the voltammetric stability of BP, PANI and BP-PANI along with the curves of ratio percentage between the final (200th) and the initial (1st) cycle of the voltammograms. The results of pure BP confirm its unstable nature, losing almost 60% of its electroactive capacity in the first few cycles. This indicates that the P oxidizes and leads to its total degradation. Regarding PANI and BP-PANI, electrochemical response losses after 200 cycles are around 32% and 24%, respectively. The greater stability of the composite may be related to BP stabilizing the PANI chains, preventing their crosslinking and consequent reduction of the electrochemical efficiency of the polymer (Fig. S2A, ESI†).[17,26]

The Raman spectra of both BP and the BP-PANI composite before and after 200 voltammetric cycles are presented in Fig. 1C and D. In general, the results show that pure BP degrades while BP covered by PANI in the composite remains intact even after 200 cycles of constant exposition to water and oxygen. Typical BP bands at 363 cm^{-1}, 440 cm^{-1} and 468 cm^{-1}, corresponding to the active modes A_g^1, B_{2g} and A_g^2,[6] are present both in the BP and BP-PANI film spectra. Also, it is possible to detect the characteristic bands of PANI in its conducting form in the BP-PANI spectrum.[17] The Raman spectra of BP (Fig. 1C) show the decrease or complete disappearance of the BP bands after 200 cycles, implying its expected poor stability. When comparing the Raman spectra of BP-PANI before and after the stability evaluation (Fig. 1D), the BP bands remain unchanged, and few changes are identified in the intensities of the 1196 cm^{-1} and 1172 cm^{-1} PANI-bands, due to an increases of its bipolaronic structure.[26]

Fig. 2A presents the X-ray diffractograms of BP-PANI before and after the cycles, evidencing in both cases the peaks related to the planes (020) and (004) of orthorhombic BP,[27] confirming the preservation of BP incorporated into the polymeric matrix. No patterns of PANI were verified, which could be related to low crystallinity of the polymer. By comparing the material before and after the cycles, a new peak at around $2\theta = 33°$ (dark circle) appears, which could indicate NaP formation (JCPDS 321143). In addition, the broadening of the peak corresponding to the (020) plane, from FWHM = 0.14 to 0.18, may indicate the intercalation of Na^+ ions into the BP lattice, suggesting that the sodiation mechanism with BP follows both processes.[25] Fig. 2B–E present the EDS spectrum along with SEM images of BP-PANI and BP after 200 cycles. Morphological characterization of the materials corroborates with the low stability of bare BP, in which only a few flakes with strong signs of degradation (arrows in Fig. 2E) were found. The SEM images confirm the BP integrity in the composite (Fig. 2C and D). EDS attested BP and PANI presence showing the peaks referring to C and P, corresponding to the proposed structure of the composite, and Na, suggesting the ion insertion into the BP-PANI structure or NaP formation. No peaks related to Cl were identified.

Given the high stability of BP covered by PANI,[17] promising electrochemical properties can be inferred from the composite even at a deeply harmful environment for the material (*i.e.* aerated water). So, we have evaluated the BP-PANI composite as an electrode for aqueous sodium batteries through charge/discharge (CD) measurements in an aqueous solution of NaCl. The specific capacities were obtained through the CD curves and the mass normalization by the entire active material.

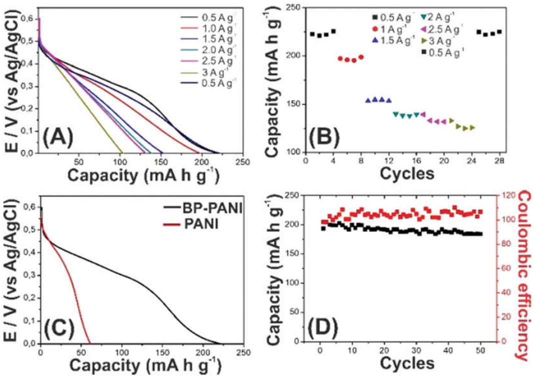

Fig. 3 (A) CD curves and (B) capacities at different applied current densities of BP-PANI, (C) CD curves of PANI and BP-PANI and (D) capacity retention and coulombic efficiency of BP-PANI cycling at 0.5 A g^{-1}. Aqueous solution NaCl 0.5 mol L^{-1} pH 3.

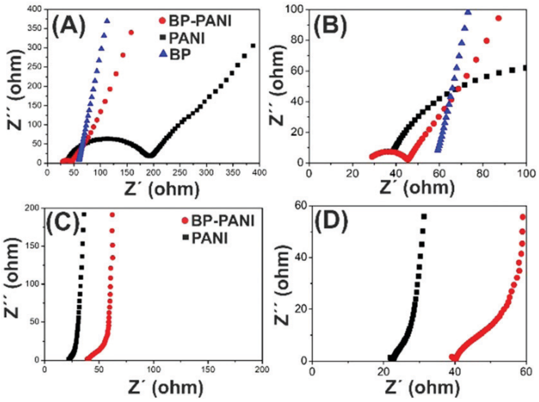

Fig. 4 Nyquist plots of samples obtained at 0.4 V in (A and B) NaCl 0.5 mol L^{-1} pH 3 and (C and D) HCl 1 mol L^{-1}.

Fig. 3A shows CD curves of BP-PANI with different applied current densities that led to the capacities exhibited in Fig. 3B. Clearly, the rate increase leads to the decay in the capacity, evidencing a well-known behaviour of battery type materials.[3] By cycling at 0.5 A g^{-1}, the BP-based composite achieved outstanding capacities of around 200 mA h g^{-1} that remain impressive (120 mA h g^{-1}) even at a higher rate of 3 A g^{-1}. When the rate was restored to 0.5 A g^{-1} after this high current application, the specific capacity of the electrode reverted to the original capacity, indicating good reversibility.

BP-PANI presented capacities almost 4 times higher than that of pure PANI, as observed through the curves in Fig. 3C. Bare BP, possibly due to its high instability in this medium, performed so poorly that no values were calculated. Fig. 3D shows that the high capacity of the BP-PANI was retained after 50 cycles, accounting for 90% of the capacity from the first cycle and an average coulombic efficiency of ≅100%.

The CD measurements and capacity values of the control samples are presented in the ESI† (Fig. S3), along with the characterization of BP-PANI after 50 cycles of CD (Fig. S4, ESI†). The SEM images show different BP flakes, with no apparent damage, spread throughout the film. EDS elemental mapping attested the integrity of BP covered by PANI evidencing a very low concentration of oxygen through the mapped BP.

The described results are notable and stand out from other literature results for similar conditions. The electrodes based on PANI have shown capacities of 180 mA h g^{-1} [20] and 280 mA h g^{-1} at 0.2 A g^{-1} for aqueous zinc batteries.[21] Concerning sodium-ion electrolytes, Kisuk Kang *et al.*[28] have reported cathodes delivering capacities of around 100 mA h g^{-1} at 1C with $NaClO_4$ aqueous electrolytes. Thus, the specific capacity of BP-PANI is attested to be among the highest reported for these aqueous systems. We believe that, in fact, several factors may be contributing to this impressive performance of the BP-PANI composite. Acting as a stabilizer for PANI chains, BP guarantees a more polaronic polymer and benefits greater internal proton storage capability, once H^+ is available.[20] Besides, the composite counts on the contribution of the energy storage mechanisms of BP itself, which may range from hosting Na^+ ions, as discussed above, to accumulating electrostatic charges on the surface.[29]

Thus, to further explore the driving force of BP, PANI and BP-PANI performance as electrodes for an aqueous sodium battery, electrochemical impedance spectroscopy (EIS) was performed in terms of Nyquist plots. In addition, to assess the electrode kinetics regarding the ion effect, we analysed the materials both in NaCl and HCl solutions, as depicted in Fig. 4.

The Nyquist curves exhibit a semicircle in the high-frequency region, representing electron transfer impedance, and an inclined line in low-frequency regions, related to ion diffusion impedance. Thus, the semicircle diameter indicates the charge transfer resistance at the cathode surface and the slope of the straight line gives information about the ionic diffusion through the lattice of the active material.[30]

Fig. 4A and B exhibit the acquired profiles, for the composite BP-PANI and control samples of BP and PANI in NaCl solution. The obtained curve for pure BP indicates a behavior with no apparent charge transfer resistance, which indicates great ionic and electronic conductivity, as previously reported for this material.[31] Regarding the composite and the neat polymer, however, the curves presented a semicircle followed by a linear profile. It is evident that the intercept and diameter of the semicircle of the BP-PANI electrode is much smaller than that of PANI, suggesting a better charge transfer kinetics. In addition, the slope of the declined line for the composite is much larger than that of PANI, indicating enhanced ion diffusion. Indeed, the lower resistance and improved diffusion properties of the BP-PANI electrode ensure a prominent rate performance,[30] corroborating with the CD results.

As the electrochemical processes were evaluated in aqueous and acidic medium, it is important to consider that a proton might be a competitive ion to Na^+. Thus, it seemed necessary to investigate the acidity effect on Na^+ intercalation into BP-PANI for the aqueous battery. For this purpose, we have also obtained the Nyquist curves in HCl 1 mol L^{-1} for BP-PANI and, as a matter of comparison, for pure PANI. The profiles presented in Fig. 4C and D show vertical lines in the low-frequency region and discrete arcs in the high-frequency region. A similar inclination of the straight lines indicates similar H^+ diffusion for PANI and

BP-PANI, and the similar arcs suggest a low electronic resistance for both materials.[32] Herein, in this case, the insertion/expulsion process of the ionic species is possibly influencing the charge compensation in PANI in the same way, in both materials, regardless of BP presence.

Thus, we can verify the interference and participation of the Na-ion in the processes involving BP-PANI electrodes, corroborating the results discussed previously (Fig. 1). Possibly, if only protons played a role when BP-PANI was evaluated in NaCl solution, both the composite and the pure polymer would behave the same way, just as it was in HCl.

In summary, a BP-PANI thin film was investigated as a candidate cathode material for a rechargeable aqueous sodium battery for the first time, using an ordinary electrolyte – NaCl solution. Unprecedentedly, we have demonstrated the high electrochemical stability of the BP-based material in its most aggressive environment: water and oxygen. The unique structure of BP covered by PANI delivered impressive capacities of almost 200 mA h g^{-1} under 0.5 A g^{-1} even after 50 cycles, while pure BP was so unstable that no measurements could be recorded. The BP integrity was monitored and attested in the composite, certifying its performance in the processes. These films can be easily tailored to the most appropriate designs aiming at energy storage devices, *e.g.* several layers can be superimposed leading to higher energy storage. Here, we have shown the feasibility of employing these materials in more environmentally friendly and low-cost systems. Thus, we believe that this work sheds light on the application of stable and reliable BP-based materials in this promising energy field.

The authors acknowledge the financial support from UFPR, CNPq, CAPES, National Institute of Science and Technology of Carbon Nanomaterials (INCT-Nanocarbon), PhosAgro/UNESCO/IUPAC and L'Oréal-UNESCO-ABC. S. H. D. thanks FAPESP (SPEC 2012/20529-8 and 2017/21988-5) for the financial support. J. E. S. F. thanks CAPES for the fellowship.

Conflicts of interest

The authors declare no conflicts of interest.

Notes and references

1 J. Liu, C. Xu, Z. Chen, S. Ni and Z. X. Shen, *Green Energy Environ.*, 2018, **3**, 20–41.
2 L. Chen, Q. Gu, X. Zhou, S. Lee, Y. Xia and Z. Liu, *Sci. Rep.*, 2013, **3**, 1946.
3 S. Husmann and A. J. G. Zarbin, *Electrochim. Acta*, 2018, **283**, 1339–1350.
4 I. Sultana, M. M. Rahman, T. Ramireddy, Y. Chen and A. M. Glushenkov, *J. Mater. Chem. A*, 2017, **5**, 23506–23512.
5 L. Chen, G. Zhou, Z. Liu, X. Ma, J. Chen, Z. Zhang, X. Ma, F. Li, H.-M. Cheng and W. Ren, *Adv. Mater.*, 2016, **28**, 510–517.
6 H. Liu, A. T. Neal, Z. Zhu, Z. Luo, X. Xu, D. Tománek and P. D. Ye, *ACS Nano*, 2014, **8**, 4033–4041.
7 S. Lin, Y. Li, J. Qian and S. P. Lau, *Mater. Today Energy*, 2019, **12**, 1–25.
8 J. Ni, L. Li and J. Lu, *ACS Energy Lett.*, 2018, **3**, 1137–1144.
9 Y. Huang, J. Qiao, K. He, S. Bliznakov, E. Sutter, X. Chen, D. Luo, F. Meng, D. Su and J. Decker, *Chem. Mater.*, 2016, **28**, 8330–8339.
10 E. Passaglia, F. Cicogna, F. Costantino, S. Coiai, S. Legnaioli, G. Lorenzetti, S. Borsacchi, M. Geppi, F. Telesio, S. Heun, A. Ienco, M. Serrano-Ruiz and M. Peruzzini, *Chem. Mater.*, 2018, **30**, 2036–2048.
11 D. Li, A. E. D. R. Castillo, H. Jussila, G. Ye, Z. Ren, J. Bai, X. Chen, H. Lipsanen, Z. Sun and F. Bonaccorso, *Appl. Mater. Today*, 2016, **4**, 17–23.
12 Z. Guo, S. Chen, Z. Wang, Z. Yang, F. Liu, Y. Xu, J. Wang, Y. Yi, H. Zhang, L. Liao, P. K. Chu and X.-F. Yu, *Adv. Mater.*, 2017, **29**, 1703811.
13 C. Xing, G. Jing, X. Liang, M. Qiu, Z. Li, R. Cao, X. Li, D. Fan and H. Zhang, *Nanoscale*, 2017, **9**, 8096–8101.
14 M. B. Erande, M. S. Pawar and D. J. Late, *ACS Appl. Mater. Interfaces*, 2016, **8**, 11548–11556.
15 M. Qiu, Z. T. Sun, D. K. Sang, X. G. Han, H. Zhang and C. M. Niu, *Nanoscale*, 2017, **9**, 13384–13403.
16 Y. Zhou, M. Zhang, Z. Guo, L. Miao, S.-T. Han, Z. Wang, X. Zhang, H. Zhang and Z. Peng, *Mater. Horiz.*, 2017, **4**, 997–1019.
17 J. E. S. Fonsaca, S. H. Domingues, E. S. Orth and A. J. G. Zarbin, *Sci. Rep.*, 2017, **7**, 10165.
18 J. Zhu, A. N. Gandi and M. Gu, *Mater. Today Energy*, 2018, **10**, 141–145.
19 H. Han, H. Lu, X. Jiang, F. Zhong, X. Ai, H. Yang and Y. Cao, *Electrochim. Acta*, 2019, **301**, 352–358.
20 H.-Y. Shi, Y.-J. Ye, K. Liu, Y. Song and X. Sun, *Angew. Chem., Int. Ed.*, 2018, **57**, 16359–16363.
21 J. Huang, Z. Wang, M. Hou, X. Dong, Y. Liu, Y. Wang and Y. Xia, *Nat. Commun.*, 2018, **9**, 2906.
22 L. Wang, Z. Sofer and M. Pumera, *ChemElectroChem*, 2015, **2**, 324–327.
23 E. Edison, S. Sreejith, C. T. Lim and S. Madhavi, *Sustainable Energy Fuels*, 2018, **2**, 2567–2582.
24 M. Mortazavi, Q. Ye, N. Birbilis and N. V. Medhekar, *J. Power Sources*, 2015, **285**, 29–36.
25 K. Hembram, H. Jung, B. C. Yeo, S. J. Pai, S. Kim, K.-R. Lee and S. S. Han, *J. Phys. Chem. C*, 2015, **119**, 15041–15046.
26 R. V. Salvatierra, M. M. Oliveira and A. J. G. Zarbin, *Chem. Mater.*, 2010, **22**, 5222–5234.
27 J. Jin, Y. Zheng, S.-z. Huang, P.-p. Sun, N. Srikanth, L. B. Kong, Q. Yan and K. Zhou, *J. Mater. Chem. A*, 2019, **7**, 783–790.
28 M. H. Lee, S. J. Kim, D. Chang, J. Kim, S. Moon, K. Oh, K.-Y. Park, W. M. Seong, H. Park, G. Kwon, B. Lee and K. Kang, *Mater. Today*, 2019, **29**, 26–36.
29 S. Wu, K. S. Hui and K. N. Hui, *Adv. Sci.*, 2018, **5**, 1700491.
30 Y. Jiao, A. Mukhopadhyay, Y. Ma, L. Yang, A. M. Hafez and H. Zhu, *Adv. Energy Mater.*, 2018, **8**, 1702779.
31 R. He, J. Hua, A. Zhang, C. Wang, J. Peng, W. Chen and J. Zeng, *Nano Lett.*, 2017, **17**, 4311–4316.
32 M. Liu, Y.-E. Miao, C. Zhang, W. W. Tjiu, Z. Yang, H. Peng and T. Liu, *Nanoscale*, 2013, **5**, 7312–7320.